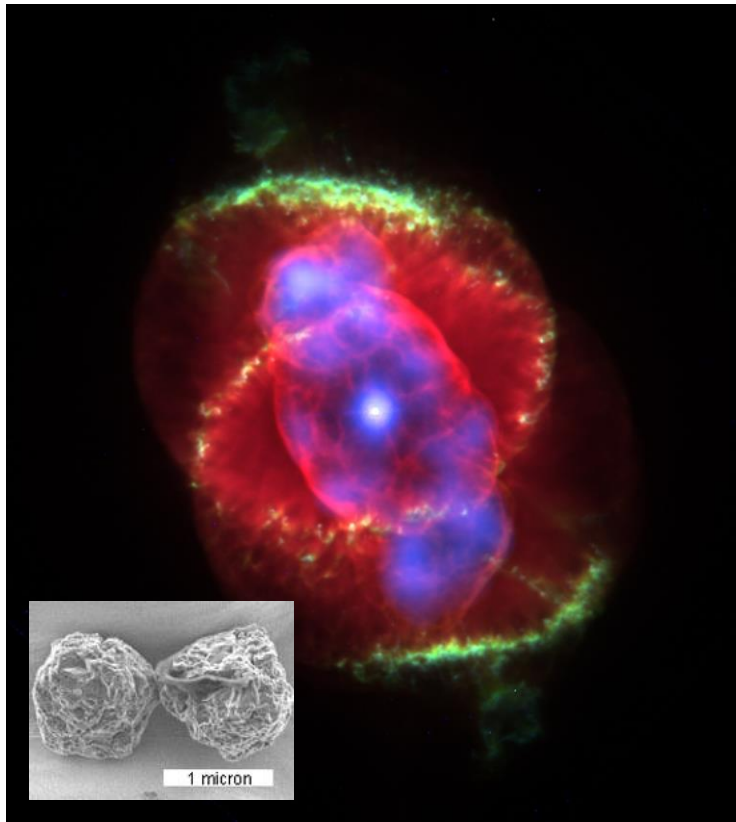
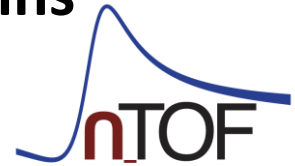




Measurement of $^{28,29,30}\text{Si}(n, \gamma)$ capture cross sections to explain isotopic abundances in presolar grains

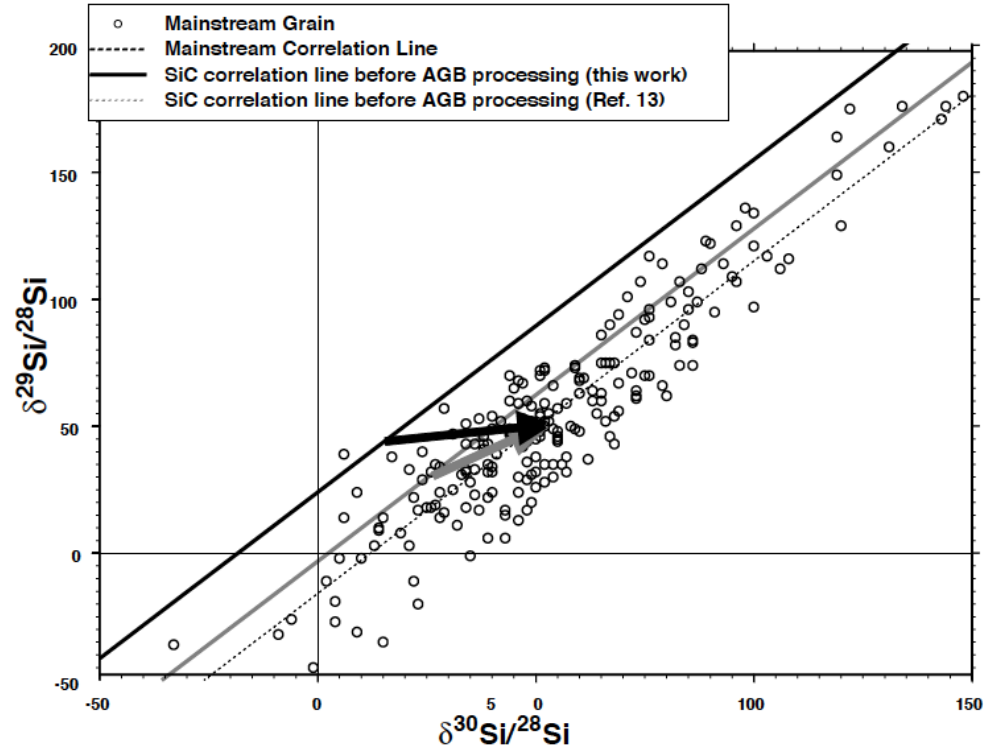
CERN-INTC-2023-009 / INTC-P-653



C. Lederer-Woods, A. Mengoni, J. Andrzejewski, M. Boromiza, A. Casanovas, S. Cristallo, M. Dietz, C. Domingo-Pardo, A. Gawlik-Ramiega, G. Gervino, A. Gugliemelli, C. Gustavino, T. Heftrich, J. Lerendegui, A. Manna, C. Massimi, A. Negret, N. Patronis, J. Perkowski, C. Petrone, M. Pignatari, T. Rauscher, R. Reifarh, A. Rooney, N. Sosnin, O. Straniero, S. Tosi, P. Ventura, D. Vescovi, P.J. Woods and the n_TOF Collaboration



- form in circumstellar envelope of AGB stars
- Si abundances: neutron capture nucleosynthesis (s process) superimposed on initial composition
- isotopic ratios measured with 5% accuracy



PHYSICAL REVIEW C 67, 062802R(2003)

→ need equally accurate neutron capture cross sections on $^{28,29,30}\text{Si}$

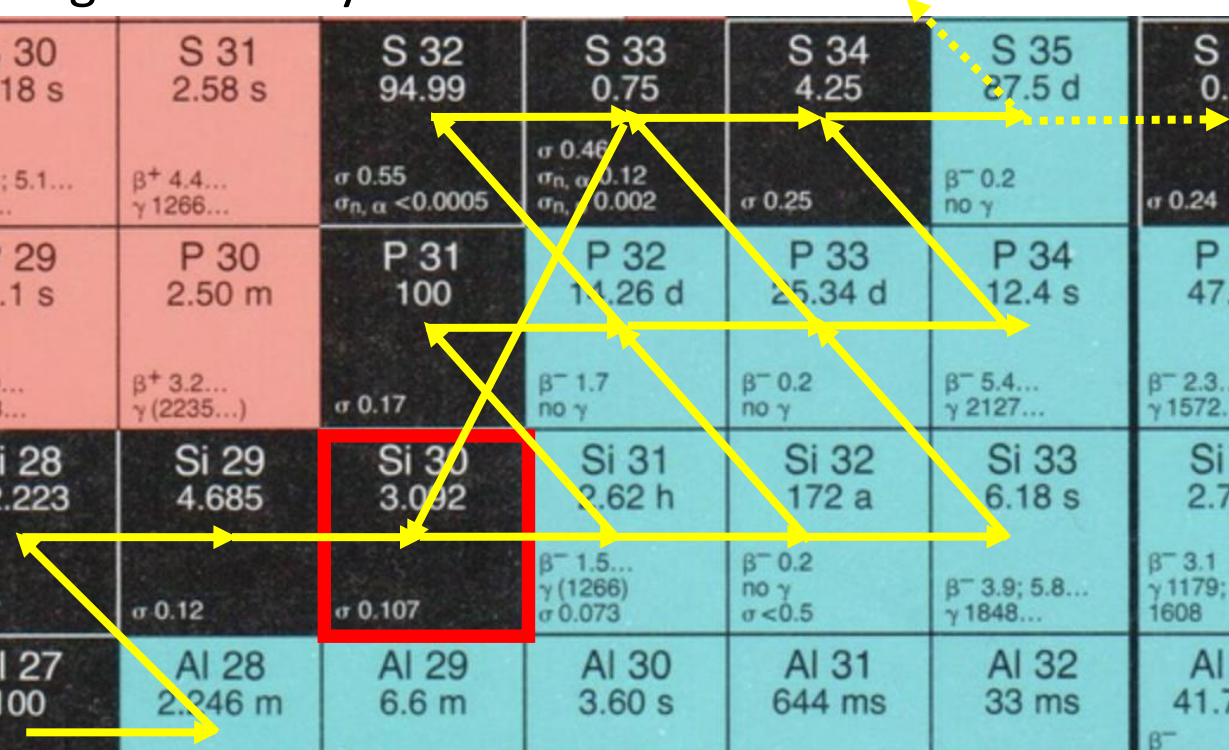


SiC Grains Type C

- C-type sub-group
- likely Supernova origin
- peculiar enhancement of ^{32}S that can be explained by presence of unstable ^{32}Si in the SN ejecta
- but needs high n-density to overcome unstable ^{31}Si



S 29 187 ms β^+ γ 1384... β_p 5.44; 2.13...	S 30 1.18 s β^+ 4.4; 5.1... γ 678...	S 31 2.58 s β^+ 4.4... γ 1266...	S 32 94.99 σ 0.55 $\sigma_{n, \alpha} < 0.0005$	S 33 0.75 σ 0.46 σ_n, α 0.12 σ_n, β 0.002	S 34 4.25 σ 0.25	S 35 27.5 d β^- 0.2 no γ	S 36 0.01 σ 0.24
P 28 268 ms β^+ 11.5... γ 1779; 4497... β_p 0.680; 0.956... β_α 2.105; 1.434...	P 29 4.1 s β^+ 3.9... γ 1273...	P 30 2.50 m β^+ 3.2... γ (2235...)	P 31 100 σ 0.17	P 32 14.26 d β^- 1.7 no γ	P 33 25.34 d β^- 0.2 no γ	P 34 12.4 s β^- 5.4... γ 2127...	P 35 47.4 s β^- 2.3... γ 1572...
Si 27 4.16 s β^+ 3.8... γ (2210...)	Si 28 92.223 σ 0.17	Si 29 4.685 σ 0.12	Si 30 3.092 σ 0.107	Si 31 2.62 h β^- 1.5... γ (1266) σ 0.073	Si 32 172 a β^- 0.2 no γ $\sigma < 0.5$	Si 33 6.18 s β^- 3.9; 5.8... γ 1848...	Si 34 2.77 s β^- 3.1 γ 1179; 429; 1608
Al 26 6.35 s β^+ 3.3 $\sigma_{n, \alpha}$ 0.34 $\sigma_{n, p}$ 1.97	Al 27 100 σ 0.230	Al 28 2.246 m β^- 2.9 γ 1779	Al 29 6.6 m β^- 2.5... γ 1273; 2426; 2028...	Al 30 3.60 s β^- 5.1; 6.3... γ 2235; 1263; 3498...	Al 31 644 ms β^- 5.6; 7.9... γ 2317; 1695...	Al 32 33 ms β^- γ 1941; 3042; 4230...	Al 33 41.7 ms β^- β_n γ 1941*; 4341; 1010





Galactic Chemical Evolution



- bulk of the ^{29}Si and ^{30}Si present today in the Milky Way and in the Sun are made in the convective carbon-shell in massive stars at about 1 GK
- $^{28,29,30}\text{Si}$ neutron capture cross sections are crucial to shape the final yields and the relative abundances of ^{29}Si and ^{30}Si

KADoNiS database, used in stellar models

▼ **Recommended MACS30** (Maxwellian Averaged Cross Section @ 30keV)



Total MACS at 30keV: 1.42 ± 0.13 mb

Cross sections do not include stellar enhancement factors!

▼ **History**

Version	Total MACS [mb]	Partial to gs [mb]	Partial to isomer [mb]
0.2	1.42 ± 0.13	-	-
0.0	2.9 ± 0.3	-	-

(Version 0.0 corresponds to Bao et al.)

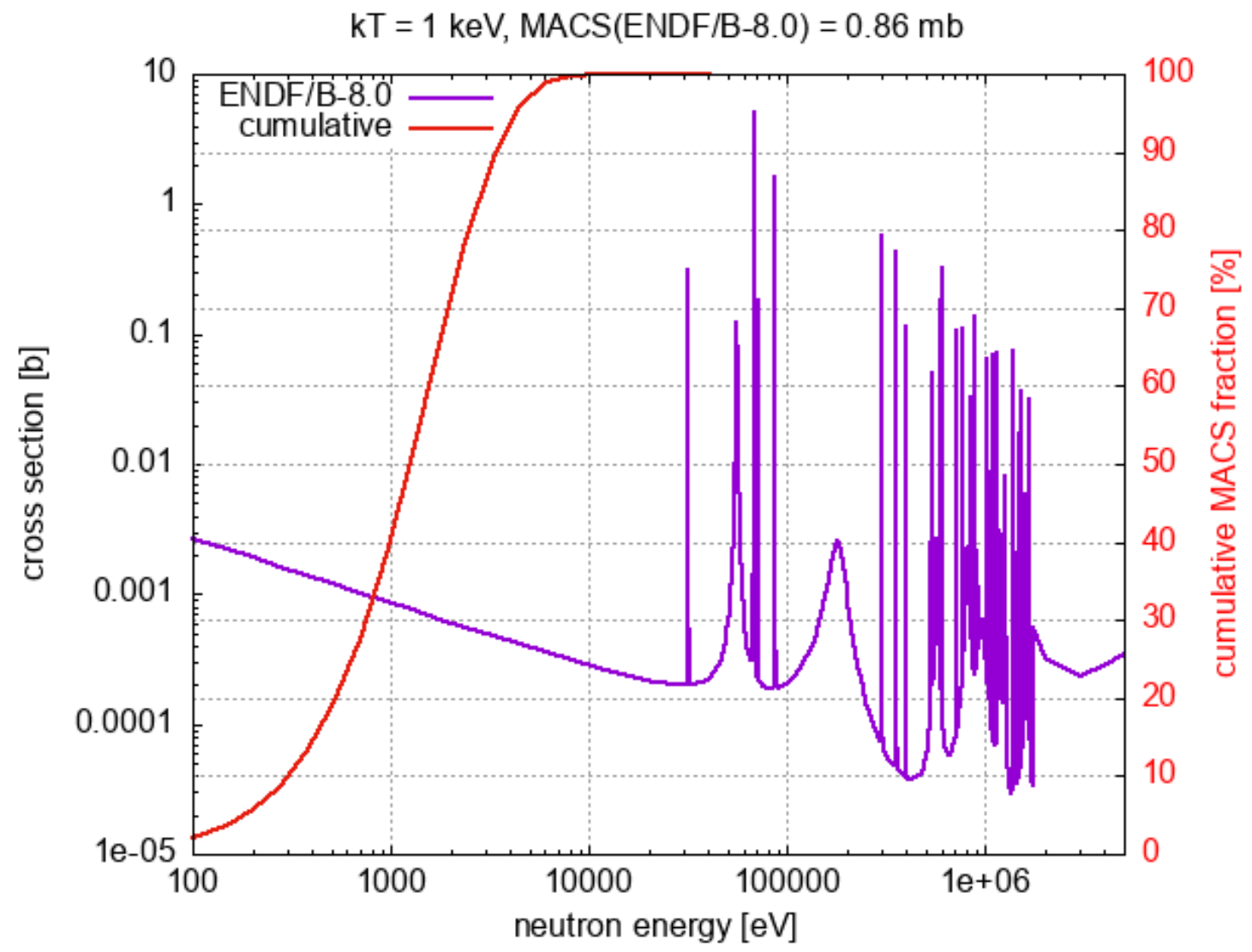
▼ **Comment**

Rec. value is from [GKD03](#). MACS vs. kT table from [GKD03](#), but extended above kT= 50 keV with norm. energy dependence from [KAB76,BAM75b](#).
Last review: February, 2013

▼ **List of all available values**

original	renorm.	year	type	Comment	Ref
1.42 ± 0.13		2003	c	Linac, TOF, Au: Sat.; DC component is 0.23 (11) mb	GKD03
2.9 ± 0.3		1976	r	Linac, TOF, ^6Li , Au:Sat. Recalcul. including data of MDH81	KAB76,BAM75b
2.9 ± 1.0		1971	e		AGM71
3.61 ± 0.80		2011	e	ENDF/B-VII.1 plus covariances	endfb71
3.61		2011	e	JENDL-4.0	jendl40
3.61		2004	e	JEFF 3.1	jeff31
1.69		2002	e	JENDL-3.3	jendl33
5.81		2015	t	TENDL-2015 using the TALYS code	tendl15
18.9		2005	t	MOST 2005	Gor05
30.8		2002	t	MOST 2002	Gor02
5.48		2000	t	NON-SMOKER	RaT99
2.4		1978	t		WFH78







▼ **Recommended MACS30** (Maxwellian Averaged Cross Section @ 30keV)



Total MACS at 30keV: 7.56 ± 0.59 mb

Cross sections do not include stellar enhancement factors!

▼ **History**

Version	Total MACS [mb]	Partial to gs [mb]	Partial to isomer [mb]
1.0	7.56 ± 0.59	-	-
0.2	6.58 ± 0.66	-	-
0.0	7.9 ± 0.9	-	-

(Version 0.0 corresponds to Bao et al.)

▼ **Comment**

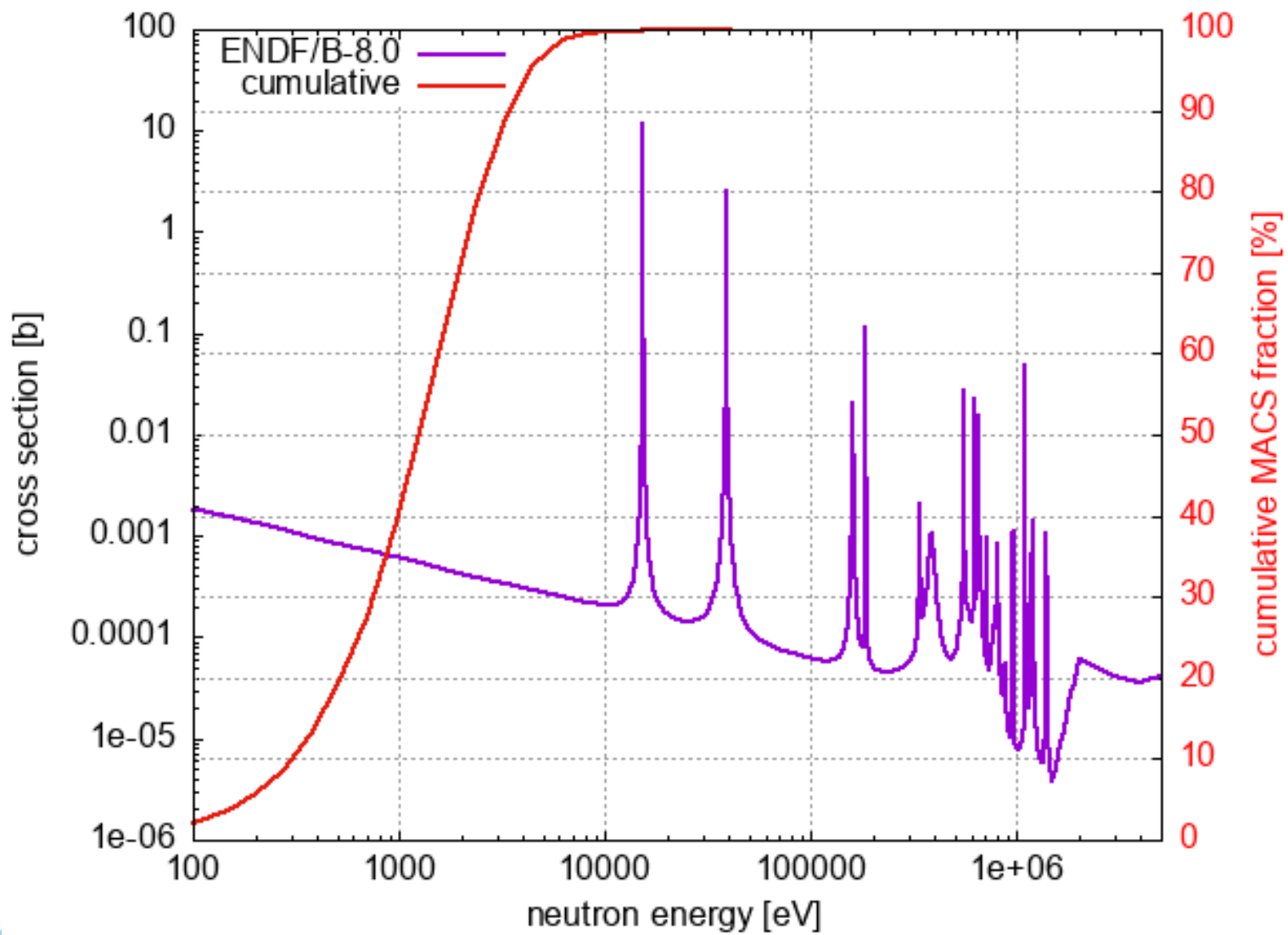
Rec. value is from [GKD03](#) (previous rec. value included no DC component). MACS vs. kT table from [GKD03](#), but extended above kT= 50 keV with norm. energy dependence from [KAB76,BAM75b](#).
Last review: February, 2013

▼ **List of all available values**

original	renorm.	year	type	Comment	Ref
7.56 ± 0.59		2003	c	Linac, TOF, Au: Sat.; DC component is 0.98 (69) mb	GKD03
7.9 ± 0.8		1976	r	Linac, TOF, ^6Li , Au:Sat. Recalcul. including data of MDH81	KAB76,BAM75b
10.4		1971	s		AGM71
7.77 ± 0.83		2011	e	ENDF/B-VII.1	endfb71
7.77		2011	e	JENDL-4.0	jendl40
5.75		2002	e	JENDL-3.3	jendl33
6.44		2015	t	TENDL-2015 using the TALYS code	tendl15
63.8		2005	t	MOST 2005	Gor05
89.2		2002	t	MOST 2002	Gor02
8.82		2000	t	NON-SMOKER	RaT99
5.4		1978	t		WFH78



$kT = 1 \text{ keV}$, $\text{MACS}(\text{ENDF/B-8.0}) = 0.61 \text{ mb}$





▼ Recommended MACS30 (Maxwellian Averaged Cross Section @ 30keV)



Total MACS at 30keV: 1.82 ± 0.33 mb

Cross sections do not include stellar enhancement factors!

▼ History

Version	Total MACS [mb]	Partial to gs [mb]	Partial to isomer [mb]
0.2	1.82 ± 0.33	-	-
0.0	6.5 ± 0.6	-	-

(Version 0.0 corresponds to Bao et al.)

▼ Comment

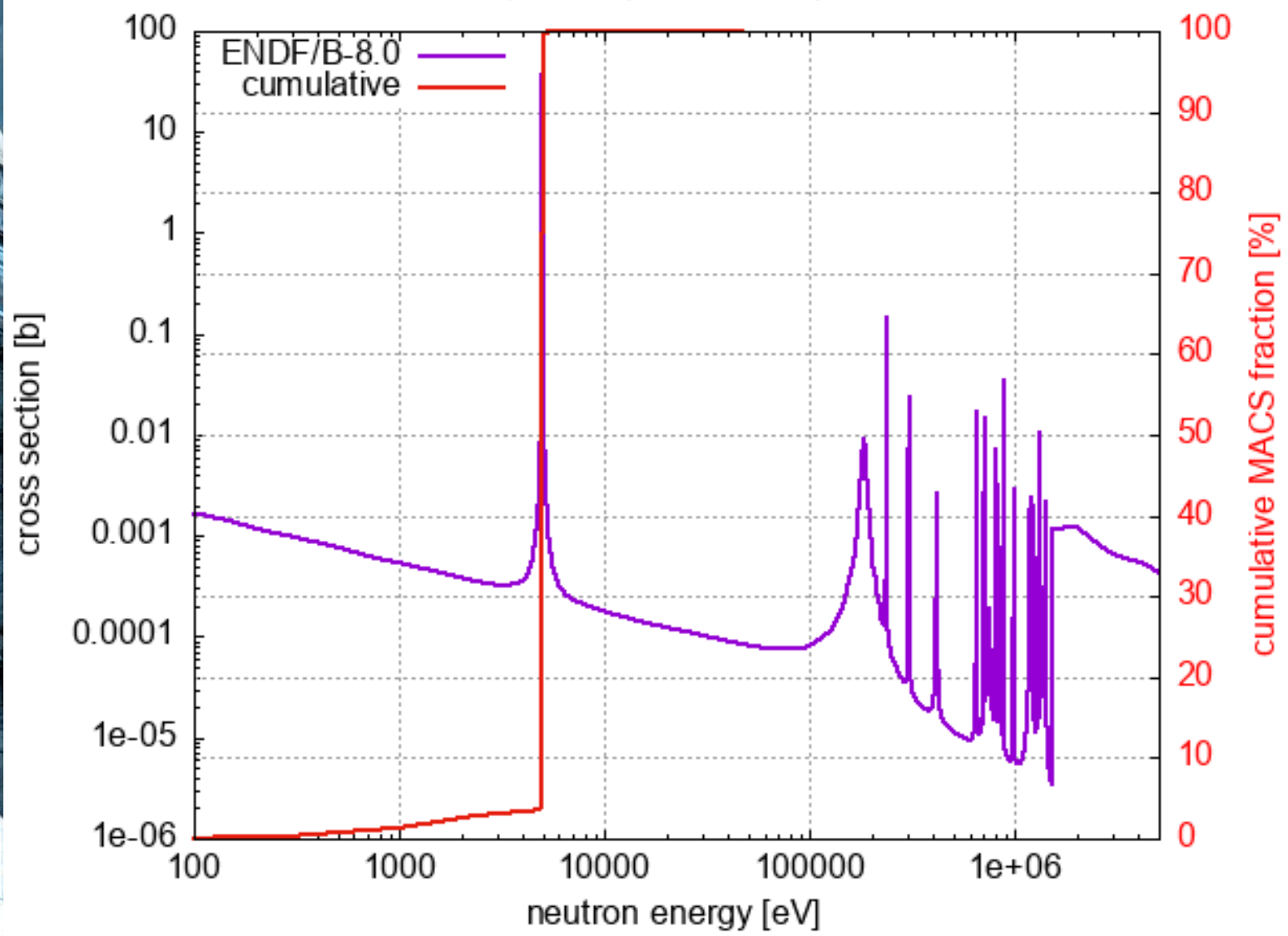
Rec. value is from [GKD03](#). MACS vs. kT table from [GKD03](#), but extended above $kT = 50$ keV with norm. energy dependence from [endfb71](#). Note that there is discrepancy between the activation measurement from [BSR02b](#) and the TOF value from [GKD03](#). **A further investigation is required!!!**
Last review: August 2014

▼ List of all available values

original	reform.	year	type	Comment	Ref
1.82 ± 0.33		2003	c	Linac, TOF, Au: Sat.; DC component is 0.48 (30) mb; no res. at 2.235 keV found	GKD03
3.51 ± 0.15 T= 25 keV	3.24 ± 0.14	2002,2015	c	VdG, Act., Au: RaK88 corrected by 632 mb/586 mb= 1.0785; DC component at $kT = 30$ keV is 0.36 mb	BSR02b
0.72 ± 0.07 kT= 52 keV		2002	c	VdG, Act., Au: RaK88	BSR02b
6.5 ± 0.6		1975	r	Linac, TOF, ^6Li , Au:Sat. Recalcul. including data of MDH81	BAM75b
1.81		2015	e	TENDL-2015 using the TALYS code	tendl15
4.43 ± 1.52		2011	e	ENDF/B-VII.1 plus covariances	endfb71
4.43		2011	e	JENDL-4.0	jendl40
5.75		2004	e	JEFF-3.1	jeff31
5.75		2002	e	JENDL-3.3	jendl33
1.9		1971	e		AGM71

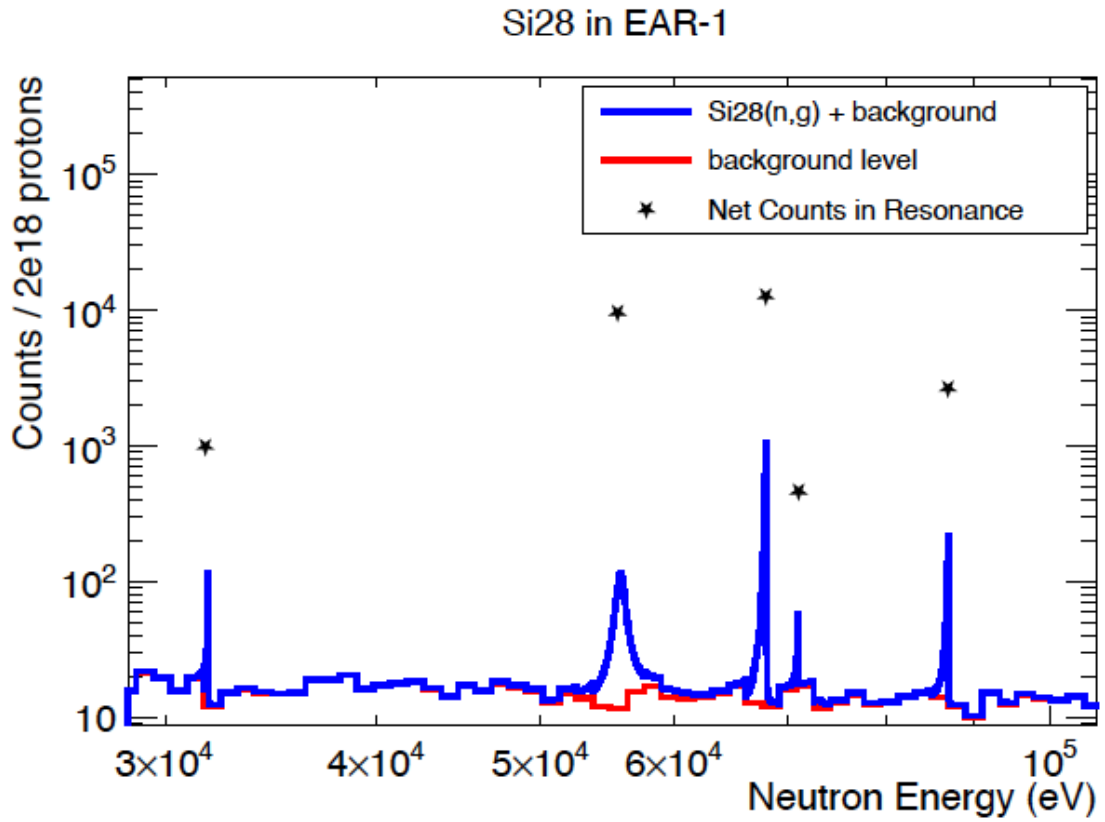


$kT = 1 \text{ keV}$, $\text{MACS}(\text{ENDF/B-8.0}) = 15.14 \text{ mb}$





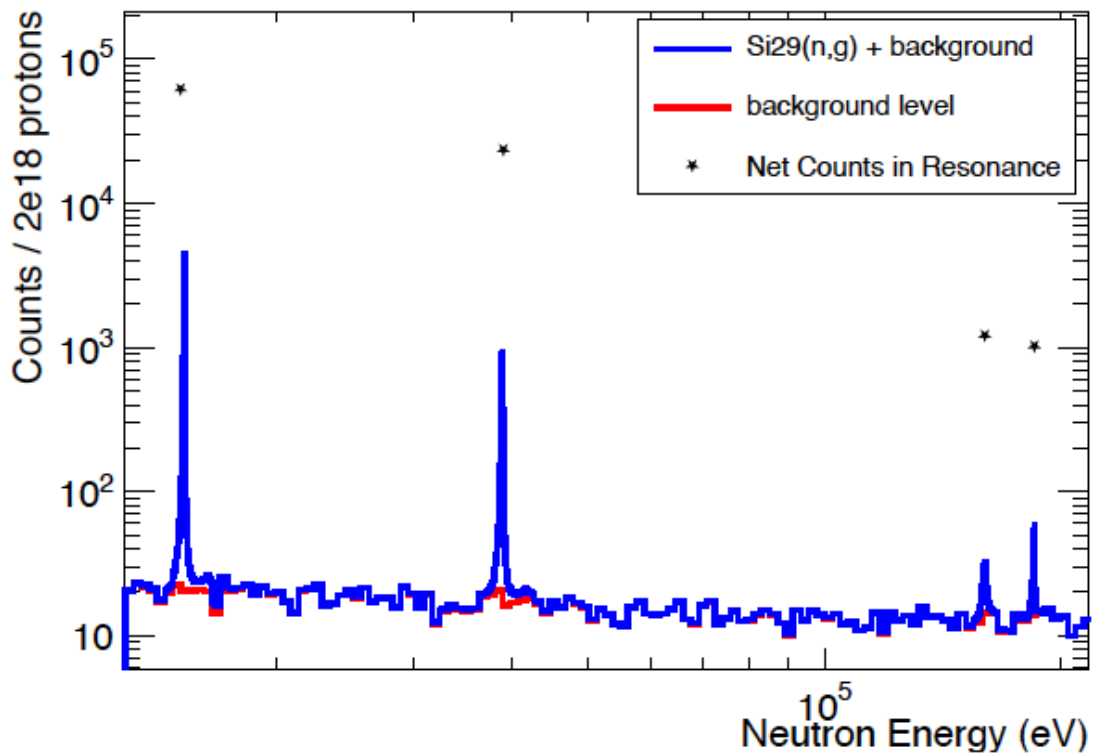
- 1g of isotopically enriched material
- Legnaro type C_6D_6 Detection Setup
- 20% cascade efficiency assumed
- $2E18$ protons





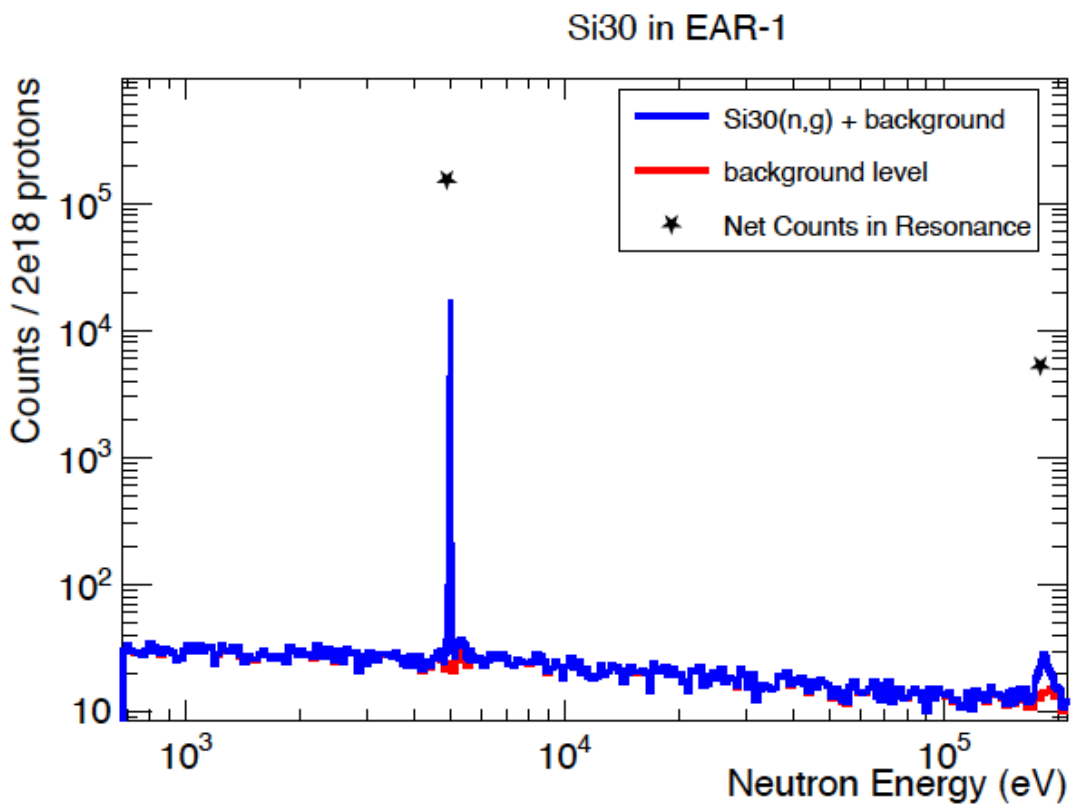
- 1g of isotopically enriched material
- Legnaro type C_6D_6 Detection Setup
- 20% cascade efficiency assumed
- $2E18$ protons

Si29 in EAR-1





- 1g of isotopically enriched material
- Legnaro type C_6D_6 Detection Setup
- 20% cascade efficiency assumed
- $2E18$ protons

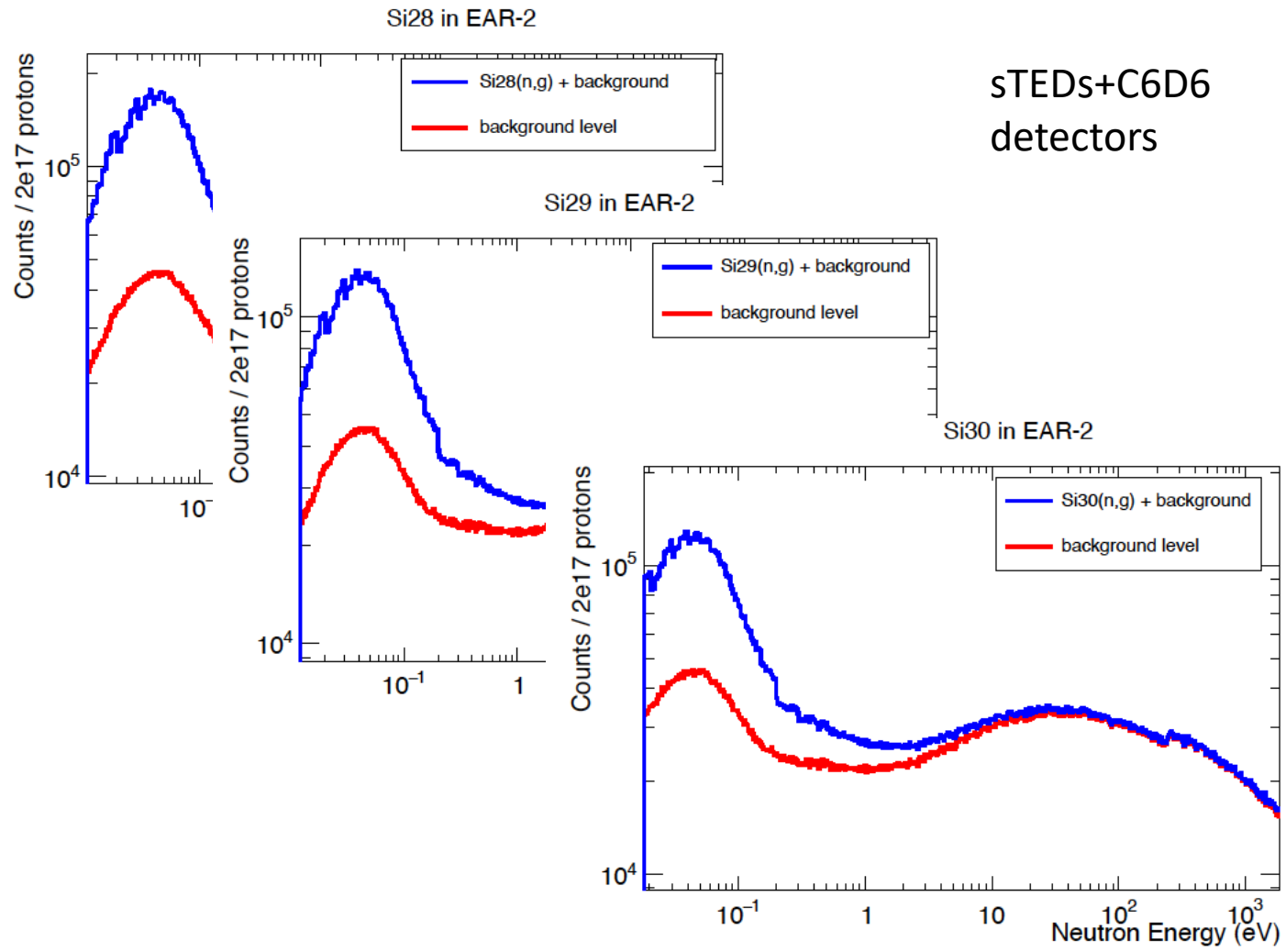




Thermal at EAR-2



sTEDs+C6D6
detectors





EAR-1

2×10^{18} protons per Si isotope

1×10^{18} protons for Au, Empty, C-nat

Total: 7×10^{18} protons

EAR-2

2×10^{17} protons per Si isotope

5×10^{17} protons for Au, Empty, C-nat

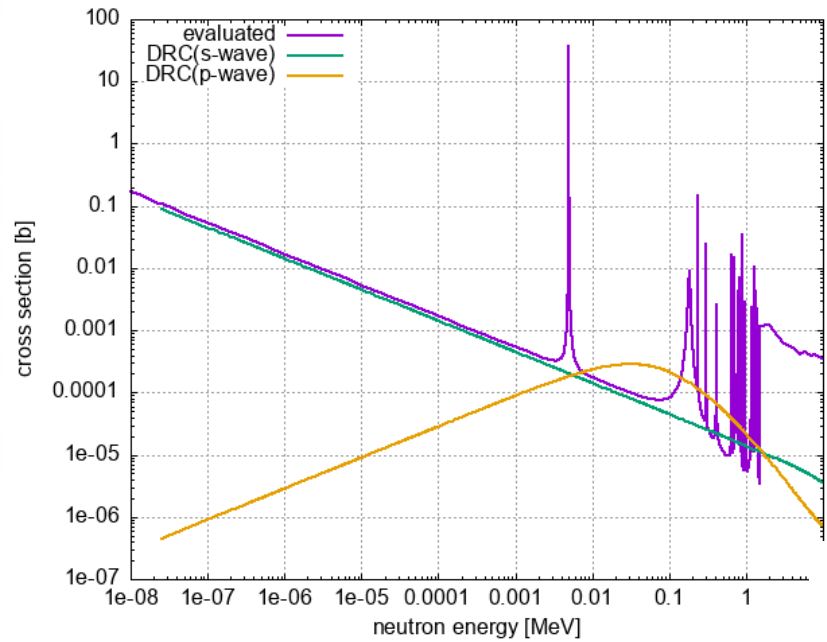
Total: 1.1×10^{18} protons



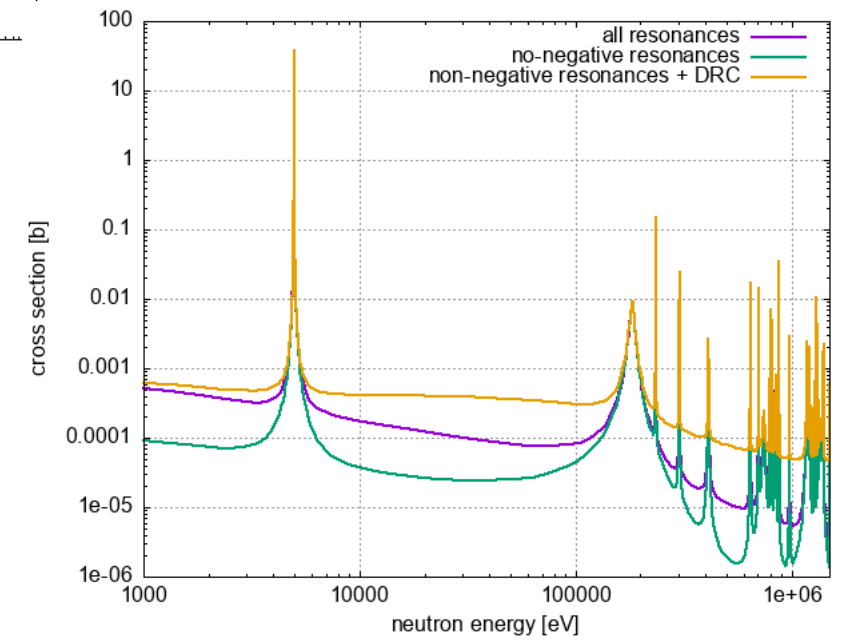
Extra slides

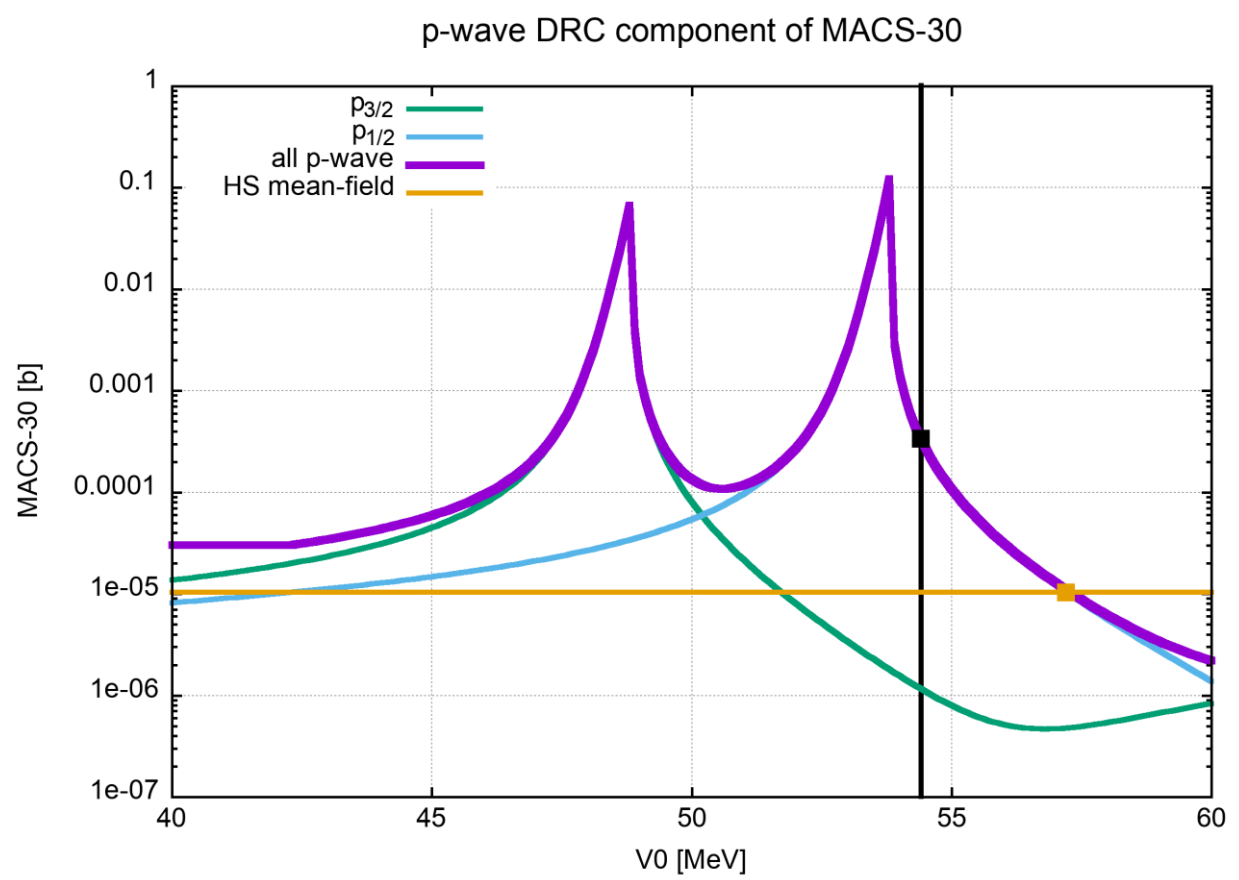


Direct Capture ^{30}Si



A. Mengoni



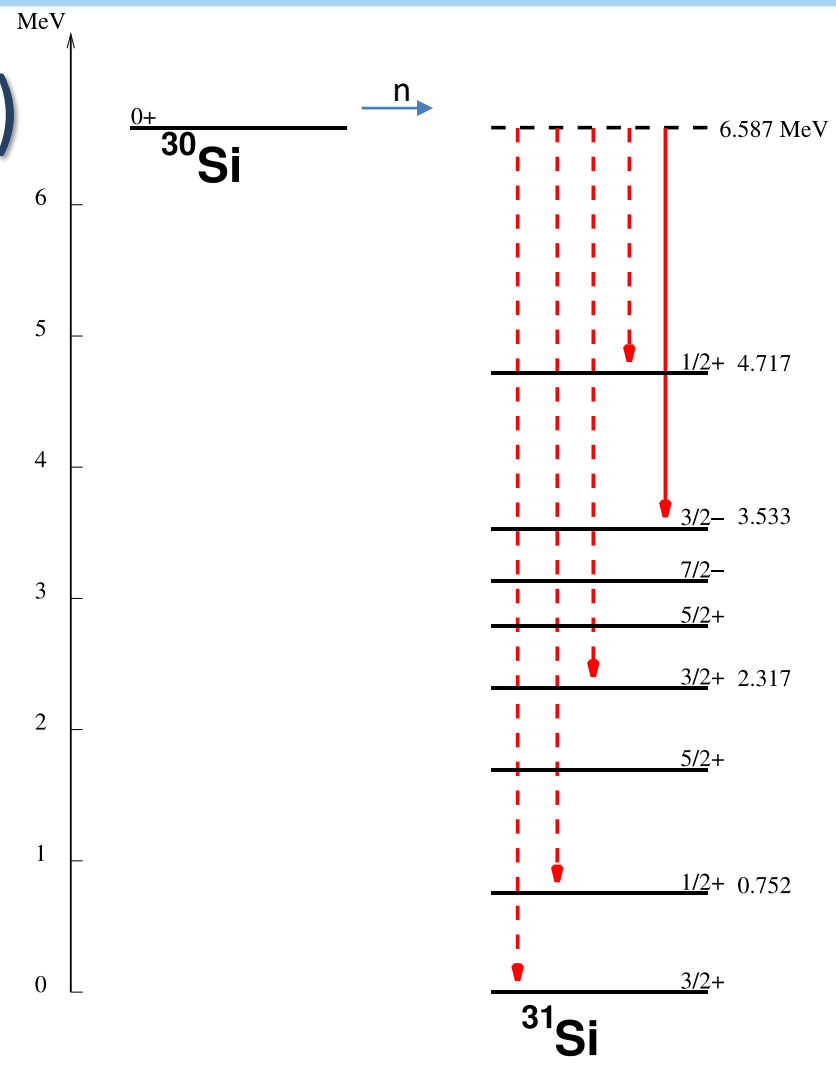


p-wave MACS-30 for Si-30. The extremely large sensitivity to the mean-field interacting potential is shown. The splitting of the 2p single-particle orbit is also apparent. The MACS-30 value obtained for a potential strength of 54.4 MeV is shown as the interception with a vertical bar, while the value for a hard-sphere potential (independent, of course, on the potential strength) is shown by the horizontal line.



$^{30}\text{Si}(n,\gamma)$

$\sigma_\gamma = 107 \pm 2 \text{ mb}$



s-wave neutrons
 M1 transitions
 ——— E1 transition

